

Sh. Aitkazinova¹,
orcid.org/0000-0002-0964-3008,
O. Sdvyzhkova^{*2},
orcid.org/0000-0001-6322-7526,
N. Imansakipova¹,
orcid.org/0000-0002-3334-645X,
D. Babets²,
orcid.org/0000-0002-5486-9268,
D. Klymenko²,
orcid.org/0000-0002-4442-9621

1 – Satbayev University, Almaty, the Republic of Kazakhstan
2 – Dnipro University of Technology, Dnipro, Ukraine
^{*} Corresponding author e-mail: sdvyzhkova.o.o@nmu.one

MATHEMATICAL MODELING THE QUARRY WALL STABILITY UNDER CONDITIONS OF HEAVILY JOINTED ROCKS

Purpose. To develop techniques for estimating the pit wall stability in terms of occurring of a zone of heavily jointed rock mass during ore mining at the Akzhal deposit (Kazakhstan), to work out measures to strengthen the rock opening and to verify the effectiveness of the developed measures.

Methodology. The finite element analysis of the rock stress-strain state is implemented on the basis of the elastic-plastic model and the generalized Hoek-Brown failure criterion. The rock mass “quality” was assessed using the RMR and GSI rating classifications. This made it possible to simulate a zone of intense fracturing by changing the characteristics of the jointed surface. The “shear strength reduction” procedure was used to determine the safety factor for the quarry wall.

Findings. The strain distributions in the rock mass forming the quarry wall have been obtained in terms of the Akzhal polymetallic ore deposit (Kazakhstan). The case of creating a zone of heavily jointed rocks in the area of a tectonic fault was considered. The safety factor of the quarry wall was determined under conditions of increased rock fracturing, as well as after carrying out measures to strengthen the rocks with a hardening solution.

Originality. The effect of intense jointness on the pit wall stability is demonstrated. A method for the consistent evaluation of the quarry wall stability is proposed considering the change in the rock properties due to natural factors and artificial reinforcement. It is shown that a change in the joint surface quality due to the hardening injection reduces the shear strains in the sliding zone.

Practical value. The pit wall stability was predicted considering the formation of a zone of intense fracturing under mining and geological conditions of the Akzhal deposit. The possibility of testing the effectiveness of rock strengthening measures based on mathematical modeling was shown.

Keywords: *quarry, wall stability, joints, rock reinforcement, finite element method, stress-strain state*

Introduction. Iron ore open pits have many problems associated with the development of the deposits and an increase in the depth of mining. The authors of [1] note that a steady decrease in the ore content in mineral deposits necessitates an increase in depth during open-pit ore mining. Therefore, steeper angles of the quarry sides are designed, which increases the risk of the slope instability and the development of sliding processes. Numerous cases of slope failure that occurred in quarries around the world require the development of a hazard assessment system based on monitoring the sides of ore quarries [2–4], as well as mathematical models for the risk evaluating [4, 5]. The slope stability estimation is mainly carried out through a combined analysis by the methods of limit equilibrium [6, 7] and numerical simulation [8, 9]. The importance of accurately replicating the pit wall contour for further numerical analysis encourages researchers to develop new analytical approaches to solving stability problems. In the work [1] mentioned above, the Dirichlet-Neumann finite element method [10] is applied, where finite elements are used in combination with the DtN mapping. The main advantage of this approach is that the Dirichlet-Neumann map provides exact boundary conditions and solution continuity when crossing an artificial boundary. This guarantees high accuracy of calculations. The article [11] presents a technique for analyzing slope stability, which combines a digital image of an object with the finite element method. This allows modeling such features of the area as complex stratigraphy, the evolution of the surface and internal geometry.

The authors of [12] point out the importance of choosing a deformation model of a rock mass and a failure criterion.

The advantages of using the Hoek-Brown failure criterion in assessing the stability of rock slopes are shown.

Identification of an unresolved problem. The above review shows that ensuring the stability of slopes and pit walls is largely determined by an adequate prediction of geomechanical processes under given geological conditions. An effective tool is mathematical, in particular, numerical modeling the stress-strain state (SSS) of a rock mass. The most proven option for SSS analysis is the finite element method (FEM) [1, 8, 11], which provides considering all the features of the rock structure. Many authors note that real cases of slope collapse in quarries are associated precisely with unforeseen alteration in the rock mass structure. Thus, the article [13] analyzes the case of an unexpected slope collapse that took place in 2016 at a copper mine in Turkey. The catastrophic event, as a result of which people died and equipment was damaged, happened due to hydrogeological regimes in the limestone-dolomite massif with a complex system of cracks. Obviously, the development of such a scenario was not foreseen at the pit design, although the authors showed such a possibility based on the limit equilibrium method. Modeling a critical situation associated with a change in the mechanical properties of rocks is demonstrated in the paper [4] in terms of an iron ore mine in Yunnan Province (China). The safety factor of the pit wall is determined under regular conditions ($SF = 1.5$), as well as under conditions of heavy precipitation ($SF = 1.21$). The results were obtained using the Midas/GTS finite element software, taking into account the results of monitoring the accumulation of precipitation and subsidence of the earth's surface throughout the year.

It follows from the above that ensuring the stability of rock openings requires an assessment of the risks associated with structural disturbances, in particular, with fracturing [14], as

well as changes in the physical and mechanical properties of rocks under the influence of natural factors. At the same time, little attention in publications is paid to methods for modeling heavily jointed parts of the slopes, which are identified while pit walls monitoring. Besides, little data is given regarding ways to increase the slope stability and strengthen the rock mass structure.

Mathematical modeling allows evaluating the effectiveness of measures aimed at rock mass strengthening, in instant, by injecting reinforcing solutions. The main difficulty lies in the correct determination of the physical and mechanical properties of the newly formed reinforced structure. There can be various approaches that combine both testing the samples of artificially maintained rocks and the use of well-approved assessments of a rock mass quality by summarizing ratings that consider various rock structure features [15].

The purpose of this work is developing a methodology for assessing the pit wall state while ore mining, as well as measures to increase the slope stability and verify the efficiency. The studies were carried out in terms of the Akzhal polymetallic ore deposit (Kazakhstan), where ensuring the pit wall stability is a vexed problem due to the complicated mining and geological conditions.

The research object description. The Akzhal deposit is located in the eastern part of the Akzhal-Aksaran shear zone and is confined to a latitudinally elongated crushing zone in the carbonate-terrigenous deposits of the Famennian and low Tournaisian. The main ore-bearing rocks are massive limestones, which are framed by siliceous limestones. The main features of the Akzhal deposit, which determined the method of development and mining technology, are the following:

- the deposit is traced along the strike for 5 km; the relief of the deposit is a ridge hillock with relative elevations up to 20 m; the ore bodies had outcrops to the day surface in the central part of the deposit;
- the ore body lies steeply to a depth of 600 m;
- the ore zone width is up to 350 m (its dip in the central part is steep and it is gently sloping in the eastern area (up to 20–30°));
- the ore-bearing and enclosing strata are represented by massive limestones and siltstones;
- the thickness of cover ore body is mainly 1–2 m, but it reaches 20–30 m in relief depressions on the western and eastern flanks of the deposit;
- there are pre-ore and intra-mineralization and post-ore disjunctives formed at different times before the occurrence of small intrusions and healed by them; they differ in size, amplitudes and intensity of accompanying rock fracturing and shearing.

A photograph and a 3D model of the Central quarry, where the main work is being carried are presented in Fig. 1. The length of the quarry on the surface is 2,860 m, the width is 820 m; bottom length is 322 m, bottom width is 30 m; the depth of the quarry is 340 m. The general slope of the pit wall at the end of mining is 43–47 degrees. The slope angle of the working ledge is 75–80 degrees.

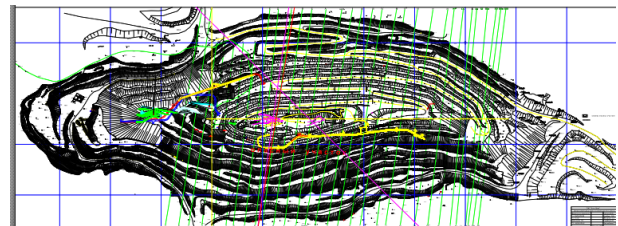
The above review shows that open pit ore mining is often accompanied by deformations of the soil and rocks, which leads to the failure of pit benches and walls in the form of landslides, shifts, scree and subsidence. The reasons for the slope failure in quarries are the discrepancy between the slope angles and geological conditions (structural and tectonic features of the rock mass and its physical and mechanical properties).

The main reasons for the failure of slopes in quarries are the following:

- unfavorable geological features, in particular, tectonic faults, change in the angle of layer dip, the presence of flooded zones and clay layers falling towards the excavation;
- change in the physical and mechanical rock properties, for instance, decrease in the rock strength at a layer contacts as a result of watering or weathering and the strength diminution over time;



a



b

Fig. 1. Quarry “Central”:

a – a photograph of the quarry; b – a 3D model of the quarry

- the negative hydrostatic and hydrodynamic impact provided by groundwater;
- the dynamic effect of mining and transport equipment, explosions and earthquakes.

Surveying observations of southern wall of Akzhal Central quarry have detected a zone of intense fracturing formed as a result of undermining a tectonic fault on the horizon of 270–320 m (Fig. 2). The revealed fault has smooth surfaces and there is a fact of its replenishment with fissure water. A system of joints is traced parallel to the identified fault.

The research purpose is to clarify the influence of the formed fracture zone on the rock stress-strain state and stability of the open pit southern side, as well as to develop preventive measures to increase the slope stability.

Research method. To determine the stress-strain state (SSS) of a rock mass, including the open pit sides, the finite element method (FEM) was used, implemented in the licensed software product PHASE2 (Rocscience). The PHASE2 code has been successfully used to simulate the geomechanical processes both in underground excavations [16] and to assess slope stability. In accordance with the FEM algorithm, all components of the stress-strain state corresponding to the terms of plane deformation are determined at the nodes of the finite element mesh and internal points of the finite elements, namely: normal σ_x , σ_y and tangential τ_{xy} stresses in the direction of the

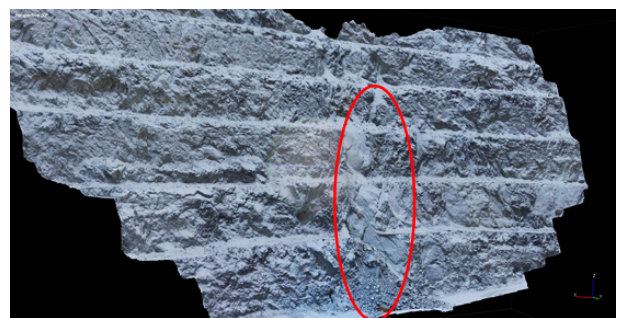


Fig. 2. The southern side of the quarry with a zone of intense fracturing on the horizon of 270–320 m

coordinate axes, principal stresses σ_1, σ_3 ($\sigma_1 > \sigma_3$), longitudinal $\varepsilon_x, \varepsilon_y$, and shear γ_{xy} strains, absolute horizontal u , and vertical v displacements. To assess the stability of slopes, the maximum shear strains are of greatest interest, since their localization determines the probable sliding curve [17].

Computing the rock deformations should be carried out within the framework of an elastic-plastic model of the solid, which provides a nonlinear relationship between stresses and strains, and is based on appropriate failure criterion. For the rocks of the Akzhal deposit, a medium model was used based on the Hawk-Brown strength criterion [11, 14, 16].

To simulate the state of Akzhal deposit rocks, the generalized Hoek-Brown failure criterion was used [11, 14, 16]

$$\sigma_1 = \sigma_3 + \sigma_c \left(m_b \frac{\sigma_3}{\sigma_c} + s \right)^a, \quad (1)$$

where σ_1, σ_3 are the maximum and minimum effective stresses at failure; σ_c is the uniaxial compressive strength of the intact rock pieces; m_b is the value of the Hoek-Brown constant m for the rock mass; s and a are constants which depend upon the rock mass characteristics (the genesis and quality of the rock mass depending on the geological strength index GSI (Geological Strength Index, $5 \leq GSI \leq 100$)). The values of the GSI are determined in accordance with the classification developed by E. Hoek and D. Brown [17]. Determining the GSI index is an especially important step, since the Hoek-Brown criterion constants are recalculated taking GSI value into account for a real jointed rock mass

$$m_b = m_i \exp\left(\frac{GSI - 100}{28 - 14D}\right); \quad (2)$$

for a rock mass of “good” quality ($GSI > 25$)

$$s = \exp\left(\frac{GSI - 100}{9 - 3D}\right), \quad a = 0.5. \quad (3)$$

Here m_i is a material constant obtained as a dependence approximation parameter $F(\sigma_1, \sigma_3) = 0$ when testing rock samples in a triaxial stress state [18], D is a factor which depends upon the degree of disturbance due to blast damage and stress relaxation. It varies from 0 for undisturbed in situ rock masses to 1 for very disturbed rock masses.

For a detailed calculation of the GSI index, other rating classifications are used, in particular, the RMR (Rock Mass Rating) developed by Z. Bieniawski [19]. It includes the following initial parameters: the uniaxial compressive strength of the intact rock; Rock Quality Designation (RQD), which is determined by the ratio of the total length of all core pieces longer than 10 cm to its total length (in percent); discontinuity spacing; condition of discontinuity surfaces; orientation of discontinuities relative to the engineered structure, and groundwater conditions. The RMR is introduced as the sum of six separate ratings, each of which corresponds to the parameters listed above

$$RMR = J_{A1} + J_{A2} + J_{A3} + J_{A4} + J_{A5} + J_{BB}. \quad (4)$$

Here $J_{A1}, J_{A2}, J_{A3}, J_{A4}, J_{A5}, J_{BB}$ are indicators (ratings) of the rock mass, which are determined for the quarry wall rocks in accordance with Table 1 based on the results of visual and instrumental examination of cores from exploratory wells and rock openings. Table 1 highlights those indicators that will be used in determining the RMR for the rocks of the southern side of the “Central” open pit.

To estimate GSI, a simple relation is proposed [20]

$$GSI = RMR - 5, \quad (5)$$

which will be used below.

The research was carried out in three stages:

- assessment of the pit wall stability before the formation of a zone of intense fracturing;

- simulation of the pit wall stability taking into account the fracturing zone formation;

- modeling the stability of the pit wall, considering measures to strengthen the rocks in the fracturing zone. At each stage, the rock mass rating RMR and the geological strength index GSI were determined, which comprehensively characterize the quality of the rock mass.

Results. Evaluation of the pit wall stability before the formation of a zone of intense fracturing. Determination of the RMR and GSI indices for the rock mass forming the southern side of the Central pit. The rock mass is composed mostly of limestone, so the geological index is determined specifically for this rock. The J_{A1} rating varies from 0 to 15 points, depending on the rock strength. The uniaxial compression strength of limestone is 80 MPa (according to the geological service of the Akzhal mining enterprise). Therefore, according to Table 1, $J_{A1} = 7$. The drilled hole core studies showed that the core recovery (RQD) is 75–90 %. Therefore, J_{A2} is taken equal to 17 points. Examination of cores and exposed rock surfaces showed that the distance between joints varies within 60–200 mm. Therefore, the J_{A3} indicator is 8 points in accordance with Table 1.

The J_{A4} rating varies from 0 to 30 points, depending on the condition of joints. The roughness of joints observed in the rock of the Central open pit are characterized as slightly rough, therefore $J_{A41} = 5$. The discontinuity length observed in the massif is 1–3 m, therefore $J_{A42} = 4$; separation varies within 1–5 mm, therefore $J_{A43} = 1$; joints are infilled with solid filler, therefore the J_{A44} rating is taken equal to 2; joints are slightly weathered, so the J_{A45} rating is taken equal to 5. In general, the J_{A4} rating of the joint condition characteristic is determined by the sum of the ratings for individual indicators

$$J_{A4} = J_{A41} + J_{A42} + J_{A43} + J_{A44} + J_{A45} = 5 + 4 + 1 + 2 + 5 = 17.$$

The J_{A5} rating varies from 0 to 15 points depending on the general groundwater conditions. This rating is assumed to be 10 (for wet surfaces). The J_{BB} rating varies from 0 to 12 points, depending on the direction of the joints relative to the outcrop. The rate of danger joints orientation is considered, too. Most of the joints observed at the mine are steeply dipping with angles of inclination $\alpha = 70^\circ$ (20.0 %), $\alpha = 80^\circ$ (17.0 %), $\alpha = 75^\circ$ (15.0 %), and $\alpha < 5 = 45^\circ$ (13.0 %). According to rate of danger, such joints are considered as “medium” and the J_{BB} rating is taken equal to 5.

Thus, for the limestone of the Akzhal deposit, the RMR quality index in accordance with (4) will be

$$\begin{aligned} RMR &= J_{A1} + J_{A2} + J_{A3} + J_{A4} + J_{A5} + J_{BB} = \\ &= 7 + 17 + 8 + 17 + 10 + 5 = 54. \end{aligned}$$

Respectively, $GSI = 49$ according to (5). Using the Rocklab program incorporated into the PHASE 2 code, the parameters of the generalized Hoek-Brown criterion (1) are determined. The parameter m_i for carbonate rocks, and therefore for limestone, is 7. Then, in accordance with (2, 3) $m_b = 0.19681$; $s = 0.00024$; $a = 0.5$.

Modeling the SSS of the pit wall before the formation of the zone of intense fracturing. The computational scheme and the finite element mesh are shown in Fig. 3. The initial data are the coordinates of the finite element mesh, as well as the limestone strength characteristics defined above.

As known [6, 7], the criterion for assessing the condition of slopes is the safety factor (SF), which is the ratio of the holding forces F_h and the shear forces F_s on the slope along the sliding surface, i. e. $SF = F_h/F_s$. If $SF > 1.0$, the slope is considered stable, $SF = 1.0$ corresponds to the limit state, which turns into collapse (shear) at $SF < 1.0$. The safety factor is determined according to “Shear Strength Reduction” procedure [7]. In accordance with it, the initial strength values decrease with a certain step until the “collapse” of the finite element model occurs. Mathematically, this means the divergence of the process of solving the resolving system of the equations.

Determination of the rock mass rating indicators for RMR [19]

| Parameter | Value intervals | | | | | | |
|--|-----------------|--------------------|----------------------|------------------|------------------|-----|----|
| A1. Uniaxial Compressive Strength (MPa) | >250 | 100–250 | 50–100 | 25–50 | 5–25 | 1–5 | <1 |
| Rating J_{A1} | 15 | 12 | 7 | 4 | 2 | 1 | 0 |
| A2. RQD (%) | 90–100 | 75–90 | 50–75 | 25–50 | <25 | | |
| Rating J_{A2} | 20 | 17 | 13 | 8 | 3 | | |
| A3. Joint Spacing, * – m ** – mm | >2* | 0.6–2* | 200–600** | 60–200** | <60** | | |
| Rating J_{A3} | 20 | 15 | 10 | 8 | 5 | | |
| A4. Condition of Joints | | | | | | | |
| A4.1. Roughness | Very rough | Rough | Slightly rough | Smooth | Slickensided | | |
| Rating J_{A41} | 6 | 5 | 3 | 1 | 0 | | |
| A4.2. Discontinuity length (persistence), m | <1 | 1–3 | 3–10 | 10–20 | >20 | | |
| Rating J_{A42} | 6 | 4 | 2 | 1 | 0 | | |
| A4.3. Separation, mm | None | <0.1 | 0.1–1.0 | 1–5 | >5 | | |
| Rating J_{A43} | 6 | 5 | 4 | 1 | 0 | | |
| A4.4. Infilling, mm | None | Hard filling <5 | Hard filling >5 | Soft filling <5 | Soft filling >5 | | |
| Rating J_{A44} | 6 | 4 | 2 | 2 | 0 | | |
| A4.5. Weathering | Unweathered | Slightly weathered | Moderately weathered | Highly weathered | Decomposed | | |
| Rating J_{A45} | 6 | 5 | 3 | 1 | 0 | | |
| $J_{A4} = J_{A41} + J_{A42} + J_{A43} + J_{A44} + J_{A45}$ | 30 | 25 | 20 | 10 | 0 | | |
| A5. Groundwater General conditions | Completely dry | damp | wet | dripping | flowing | | |
| Rating J_{A5} | 15 | 10 | 7 | 4 | 0 | | |
| B. Joint orientations | Very favorable | favorable | fair | unfavorable | Very unfavorable | | |
| Rating J_B | 0 | –2 | –5 | –10 | –12 | | |

From a geomechanical point of view, the moment of divergence of the computational process and the “collapse” of the numerical model means the loss of slope stability, and the Strength Reduction Factor (SRF) is interpreted as a safety factor (SF).

For the conditions described above, the safety factor (SF) on the left (steeper) side of the pit is 1.16. This means that rock mass sliding (the loss of stability) occurs if the strength properties are reduced by a factor of 1.16. Fig. 3 shows (lower scale) how the strength reduction factor is introduced step by step. At each step, all components of the stress-strain state are ana-

lyzed, including the maximum shear strain. As mentioned above, it is the shear deformations that are believed to be responsible for the formation of the sliding surface. Fig. 4 shows the area of concentration of maximum shear strains, corresponding to a decrease in shear strength by 1.16 (green and turquoise tones in the color scheme).

Thus, the southern side of the quarry “Central”, composed by limestones with a geological strength index $GSI = 49$, is stable in terms of limit equilibrium. At the same time the safety factor $SF = 1.16$ is lower than the factor recommended by the design standards ($SF = 1.3$).

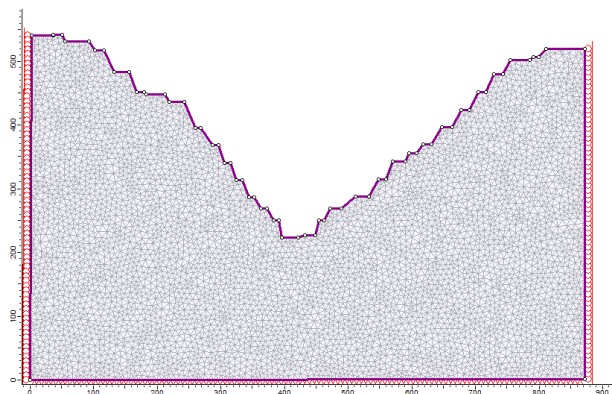


Fig. 3. The computational scheme and the finite element mesh

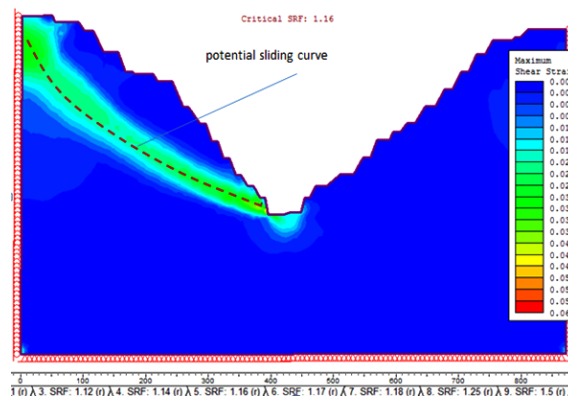


Fig. 4. Potential distribution of maximum shear strains at the moment of sliding and potential sliding curve

Considering the fracture zone formation when assessing the pit wall stability. As indicated above, an area of increased rock fracturing formed as a result of tectonic fault undermining, was recorded while monitoring the southern side of the quarry. The identified tectonic contact has a fairly smooth surface and there is a fact of its watering. Geometric parameters of the detected fracture area are 35 m in height and 20 m in width. In addition, a system of cracks parallel to the identified fault is traced at the horizons of 270–320 m.

To assess the effects of the fracture zone on the stability of the open pit side, it was included in the calculation scheme (Fig. 5).

Rock fracturing in the specified area is modeled by reducing the GSI index to a value that corresponds to a disintegrated rock mass broken by joints with smooth contact surfaces. The GSI value is calculated as described above using the RMR index.

Determination of RMR and GSI indices for a zone of increased fracturing. The J_{A1} rating remains to be 7 (it corresponds to the intact rock mass compressive strength of 80 MPa). The RQD index in this zone was determined using ultrasonic sounding. An acoustic probe with piezoelectric sensors was lowered into the drilled well discretely with an interval of 15–20 cm. The position of the probe for each measurement was fixed by a pressure pneumatic system, which provided reliable contact conditions for the piezoelectric sensors with the rock mass. The core is divided into parts along natural joints. This provides for determining the length of the core pieces and calculating the RQD index. The distances between joints are found from the delay time of the impulses reflected from the edge of each crack and recorded by the sensors. In Table 2, the lengths of the core pieces determined by the ultrasonic method for one of the three drilled wells are presented.

Pieces less than 10 cm long are not included in the RQD calculation. Then the quality index of the rock mass in accordance with Table 2 equals, %

$$RQD = \frac{\sum l_i \cdot n_i}{L} = \frac{4110}{16,506} \cdot 100\% = 24.9.$$

Similarly, the RQD indices for the second and third wells are determined, which are $RQD(2) = 33.5\%$; $RQD(3) = 45.3\%$. Then, in accordance with Table 1, the J_{A2} rating equals to 8 points.

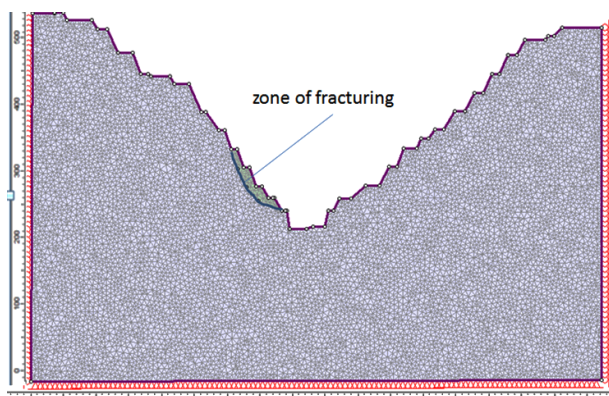


Fig. 5. Introduction to the design scheme of a fracture zone by reducing the GSI index in the specified area

Table 2

Lengths of core sections drilled in the zone of increased fracturing

| Core section length, l_i , mm | 380 | 350 | 290 | 250 | 200 | 150 |
|--|-----|-----|-----|-----|-----|-----|
| The number of pieces of the same length, n_i | 1 | 2 | 2 | 3 | 4 | 6 |

The distance between joints in the fracture zone varies within 60–200 mm. Therefore, the J_{A3} index remains unchanged and equals 8 points. The components of the J_{A4} rating in the fracture zone are as follows: J_{A41} is set equal to 0, since the walls of the joints are smooth and there are sliding surfaces. The length of the joints observed in the fracture area has increased to 10–20 m, so J_{A42} is set equal to 1. The degree of separation becomes more than 5 mm, so $J_{A43} = 0$. Joints in the fracture zone are filled with soft aggregate or not filled at all, so the J_{A44} rating is taken equal to 0. The J_{A45} rating is set equal to 1 for highly open cracks. In general, the rating of the J_{A4} fracture geological characteristic is only 2 points.

The J_{A5} rating is assumed to be 10 (for wet surfaces). The J_{BB} rating is taken equal to 5, since the degree of danger due to the direction of the joints is considered as “medium”.

Thus, for rocks in the fracture zone, the RMR index is as follows

$$RMR = J_{A1} + J_{A2} + J_{A3} + J_{A4} + J_{A5} + J_{BB} = 7 + 8 + 8 + 2 + 10 + 5 = 30.$$

Respectively, $GSI = 25$ according to (5). By Rocklab program data, incorporated in PHASE 2 code, for $GSI = 25$ the parameters of criterion (1) take values: $m_b = 0.033$; $s = 0.0000037$; $\alpha = 0.5313$.

Simulation results of pit wall stability with consideration of the fracture zone formed. The zone of fracturing reduces the stability factor of the pit wall to the value of $SF = 0.92$ (Fig. 6), which should be interpreted as the implementation of the rock masses slip and the formation of local rock falls. The color scheme shows the concentration of maximum shear strains (turquoise and green shades), which actually determines the real sliding curve for the given geological conditions. It can be seen that the real slide curve is formed along the boundary of the zone of increased fracturing. In the rest part of the slope, shear strains are an order of magnitude smaller, but in general the situation should be considered as critical, requiring the development of measures either to strengthen rocks or to change the geometric parameters of the benches in the zone of structural weakening of the rock mass.

Development of measures to strengthen the fractured zone. One of the ways to strengthen hard rocks and soils is the injection of hardening mixtures into cracks. The authors have developed a formulation of a construction hardening mixture based on the tailings of the Akzhal polymetallic ore processing. Based on the analysis of solid wastes, a hardening mixture with the following mass ratio was developed: cement is 32–37 %, tailings of concentration plants is 47–52 %, superplasticizer Neolit 400 is from 0.11 to 0.16 %, the rest is water. Laboratory tests of cement stone samples showed that the material, obtained after hardening, has strength of at least 35 MPa. Injection of grouting mortar into cracks provides their filling

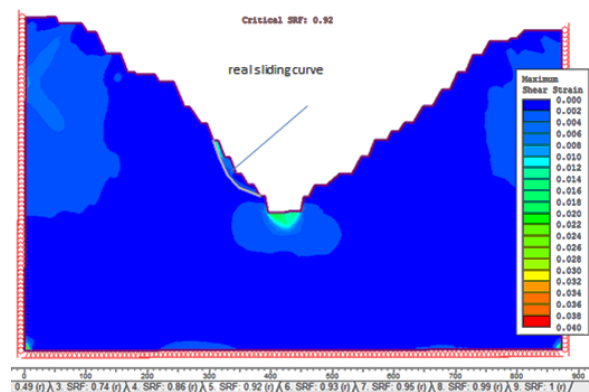


Fig. 6. Distribution of maximum shear strains at the moment of stability loss and the sliding curve in the fracture zone

with hardening material, thereby partially leveling the negative effect of fracturing in the rock mass.

Let us determine the geological strength index of the rock mass when strengthening the joints with hardening mixture. In this case, taking into account the fact that the strength of the hardening material is not less than 35 MPa, we assume the component J_{444} of the *RMR* rating to be 2 as for joints with a solid filler more than 5 mm thick. The J_{A41} rating should also be increased to a value of 1, since slip planes are eliminated due to joints infilling. Thus, the *RMR* index is increased to 33 points and the *GSI* index is increased to 28 points respectively. As *GSI* changes, the constants of the Hoek-Brown criterion change as well: $m_b = 0.041$, $s = 0.0000061$; $\alpha = 0.5$. The result of strengthening the fracture area is an increase in the stability factor to a value of 1.04. The slip curve, which could potentially form, is also in the area of fracturing, but infilling the joints increases the rock cohesion and stabilizes the deformations. The maximum shear strains at the top of the slip area with unfilled open joints are $\gamma = 0.12$ (Fig. 6). When the joints are filled with hardening mixture, the deformations in the upper part of the potential sliding surface drops to a value of $\gamma = 0.04$, i.e. three times as much.

Thus, the zone of fracturing in the rock mass, located in the area of tectonic fault, causes the instability of the pit wall, reducing the safety factor below the level of limit equilibrium. Injection of hardening mixture based on polymetallic ore tailings helps to fill joints and increase cohesion in the block structure of rocks. This enhances the ability of rocks to resist the shear components of the stress field.

It is obvious that the measures for strengthening the fractured structure cannot raise the safety factor up to the design level ($SF=1.3$). But the performed simulation shows that the fact of possible formation of fracture zones should be taken into account when designing the open pit and justifying the resulting inclination angle of the wall.

Conclusions.

1. Mathematical modeling of the rock stress-strain state is an effective component in the complex of exploration works when assessing the stability of the pit walls while ore mining. The rating technique of rock mass “quality” assessment combined with the empirical Hoek-Brown criterion provides for building a real deformation model of the environment and represents all features of the rock mass, directly affecting the stability of the pit walls.

2. According to the developed research algorithm, the southern side of the “Central” quarry, consisting of limestone with a geological index $GSI = 49$, is stable, although the stability factor of $SF = 1.16$ is below the recommended design standards ($SF = 1.3$).

3. The zone of fracturing located in the area of tectonic fault causes the instability of the pit wall. The safety factor drops not only below the design level (1.3), but also below the level of limiting equilibrium (1.0), making 0.92. The manifestation of such a condition is the occurrence of rock falls and landslides.

4. The injection of hardening mixture based on polymetallic ore tailings helps to fill fractures and increase cohesion in the block structure of rocks. This enhances the ability of rocks to resist the shear components of the stress field. The performed modeling showed that the safety factor of the pit wall rises to the value of 1.04 due to proposed measures. It is obvious that strengthening of fractured structure cannot enhance the stability reserve to the design level, however the presence of solid filling increases cohesion of rocks and provides the strain stabilization, reducing them in the zone of potential sliding by three times.

5. The simulation shows that the fact of possible formation of fault and fracture zones should be taken into account when designing the open-pit mine and justifying the resulting slope angle of the wall.

Acknowledgment. *The study was financially supported by the Science Committee of the Ministry of Education and Science of*

the Republic of Kazakhstan (Grant No. AP08053410 “Development of innovative methods for predicting and assessing the state of a rock mass to prevent technogenic emergencies” and Grant No. AR 09261035 “Development of a highly efficient system for diagnosing the stress-strain state of a rock mass and spatio-temporal analysis of the development of deformation processes throughout the deposit”).

References.

1. Durán, M., Godoy, E., Román Catafau, E., & Toledo, P. A. (2022). Open-pit slope design using a DTN-FEM: Parameter space exploration. *International Journal of Rock Mechanics and Mining Sciences*, 149, 104950. <https://doi.org/10.1016/j.ijrmms.2021.104950>.
2. Uteshov, Y., Galiyev, D., Galiyev, S., Rysbekov, K., & Nauryzbayeva, D. (2021). Potential for increasing the efficiency of design processes for mining the solid mineral deposits based on digitalization and Advanced Analytics. *Mining of Mineral Deposits*, 15(2), 102-110. <https://doi.org/10.33271/mining15.02.102>.
3. Sobko, B., Drebenstedt, C., & Lozhnikov, O. (2017). Selection of environmentally safe open-pit technology for mining water-bearing deposits. *Mining of Mineral Deposits*, 11(3), 70-75. <https://doi.org/10.15407/mining11.03.070>.
4. Yuan, L., Li, C., Li, S., Ma, X., Zhang, W., Liu, D., Wang, G., Chen, F., & Hou, X. (2022). Mine slope stability based on fusion technology of InSAR Monitoring and numerical simulation. *Scientific Programming*, 2022, 1-10. <https://doi.org/10.1155/2022/8643586>.
5. Shcherbakov, P., Tymchenko, S., Bitimbayev, M., Sarybayev, N., & Moldabayev, S. (2021). Mathematical model to optimize drilling-and-blasting operations in the process of open-pit hard rock mining. *Mining of Mineral Deposits*, 15(2), 25-34. <https://doi.org/10.33271/mining15.02.025>.
6. Su, P., Qiu, P., Liu, B., Chen, W., & Su, S. (2022). Stability prediction and optimal angle of high slope in open-pit mine based on two-Dimension Limit equilibrium method and three-dimension numerical simulation. *Physics and Chemistry of the Earth, Parts A/B/C*, 127, 103151. <https://doi.org/10.1016/j.pce.2022.103151>.
7. Li, H., Zhang, Z., & Yang, W. (2021). Stability analysis of slope based on limit equilibrium method and strength reduction method. *Annales De Chimie – Science Des Matériaux*, 45(5), 379-384. <https://doi.org/10.18280/acsm.450503>.
8. Sdvyzhkova, O., Babets, D., Moldabayev, S., Rysbekov, K., & Sarybayev, M. (2020). Mathematical modeling a stochastic variation of rock properties at an excavation design. *SGEM International Multidisciplinary Scientific GeoConference EXPO Proceedings*. <https://doi.org/10.5593/sgem2020/1.2/s03.021>.
9. Sdvyzhkova, O. O., Shashenko, O. M., & Kovrov, O. S. (2010). Modelling of the rock slope stability at the controlled failure. *Proceedings of the European Rock Mechanics Symposium – Switzerland: European Rock Mechanics Symposium, EUROCK 2010; Lausanne; Switzerland*, 581-584.
10. Godoy, E., Boccardo, V., & Durán, M. (2017). A Dirichlet-to-Neumann finite element method for axisymmetric elastostatics in a semi-infinite domain. *Journal of Computational Physics*, 328, 1-26. <https://doi.org/10.1016/j.jcp.2016.09.066>.
11. Wijesinghe, D. R., Dyson, A., You, G., Khandelwal, M., Song, C., & Ooi, E. T. (2022). Development of the scaled boundary finite element method for image-based slope stability analysis. *Computers and Geotechnics*, 143, 104586. <https://doi.org/10.1016/j.compgeo.2021.104586>.
12. Karrech, A., Dong, X., Elchalakani, M., Basarir, H., Shahin, M. A., & Regenauer-Lieb, K. (2022). Limit analysis for the seismic stability of three-dimensional rock slopes using the generalized Hoek-Brown criterion. *International Journal of Mining Science and Technology*, 32(2), 237-245. <https://doi.org/10.1016/j.ijmst.2021.10.005>.
13. Lashgari, M., & Ozturk, C. A. (2021). Slope failure and stability investigations for an open pit copper mine in Turkey. *Environmental Earth Sciences*, 81(1). <https://doi.org/10.1007/s12665-021-10125-7>.
14. Gharehdaghi, M. S., Tehrani, H., & Fakher, A. (2020). Risk-based decision making method for selecting slope stabilization system in an abandoned open-pit mine. *The Open Construction and Building Technology Journal*, 14(1), 198-217. <https://doi.org/10.2174/1874836802014010198>.
15. Kang, K.-S., Hu, N.-L., Sin, C.-S., Rim, S.-H., Han, E.-C., & Kim, C.-N. (2017). Determination of the mechanical parameters of rock mass based on a GSI system and displacement back analysis. *Journal of Geophysics and Engineering*, 14(4), 939-948. <https://doi.org/10.1088/1742-2140/aa6e78>.

16. Sdvyzhkova, O., Babets, D., Kravchenko, K., & Smirnov, A. (2015). Rock state assessment at initial stage of longwall mining in terms of poor rocks of western Donbass. *New Developments in Mining Engineering 2015: Theoretical and Practical Solutions of Mineral Resources Mining, 2015*, 65-70.
17. Zuo, J., & Shen, J. (2020). The Hoek-Brown failure criterion. *The Hoek-Brown Failure Criterion – From Theory to Application*, 1-16. https://doi.org/10.1007/978-981-15-1769-3_1.
18. Arshadnejad, Sh. (2018). Determination of “mi” in the Hoek–Brown failure criterion of rock. *Mining Science*, 25, 111-127. <https://doi.org/10.5277/msc182509>.
19. Fairhurst, C. (2014). *Analysis and Design Methods: Comprehensive Rock Engineering: Principles, Practice and Projects*. Elsevier. <https://doi.org/10.1201/b16955-9>.
20. Somodi, G., Bar, N., Kovács, L., Arrieta, M., Török, Á., & Vásárhelyi, B. (2021). Study of rock mass rating (RMR) and Geological Strength index (GSI) correlations in granite, siltstone, sandstone and quartzite rock masses. *Applied Sciences*, 11(8), 3351. <https://doi.org/10.3390/app11083351>.

Математичне моделювання стійкості борту кар'єра в умовах підвищеної тріщинуватості гірських порід

Ш. К. Айтказінова¹, О. О. Сдвижкова*²,

Н. Б. Імансакіпова¹, Д. В. Бабець², Д. В. Клименко²

1 – Satbayev University, м. Алмати, Республіка Казахстан

2 – Національний технічний університет «Дніпровська політехніка», м. Дніпро, Україна

* Автор-кореспондент e-mail: sdvyzhkova.o.o@nmu.one

Мета. Розробка методика оцінки стійкості борту кар'єру в умовах утворення зони інтенсивної тріщинуватості при відпрацюванні рудного покладу родовища Акжал (Казахстан), розробка заходів зі зміцнення порідних оголень і перевірка ефективності цих заходів.

Методика. Скінчено-елементний аналіз напружено-деформованого стану породного масиву реалізовано на основі пружно-пластичної моделі середовища та узагальненого критерію міцності Хока-Брауна. Оцінка якості породного масиву виконана з використанням рейтингових класифікацій *RMR* і *GSI*. Це дозволило змодельовати зону інтенсивної тріщинуватості шляхом зміни характеристик поверхні тріщин. Процедура «зниження зсувної міцності» використана для визначення коефіцієнта запасу стійкості борту кар'єра.

Результати. Отримано розподіл деформацій у породному масиві, що складає борт кар'єру в умовах родовища поліметалічних руд Акжал (Казахстан). Розглянуто випадок, коли в районі тектонічного розлому утворилася зона інтенсивної тріщинуватості. Визначено коефіцієнт запасу стійкості для борту кар'єру в умовах підвищеної тріщинуватості порід, а також після проведення заходів щодо зміцнення порід розчином, що твердіє.

Наукова новизна. Показано вплив утворення зони інтенсивної тріщинуватості на стійкість борту кар'єру. Запропонована методика послідовної оцінки стійкості борту кар'єру при зміні властивостей порід за рахунок природних факторів і штучного зміцнення. Показано, що зміна якості поверхні тріщин унаслідок ін'єкції розчину, що твердіє, зменшує у три рази деформації зсуву в зоні ковзання.

Практична значимість. Для гірничо-геологічних умов родовища Акжал спрогнозована стійкість борту кар'єру при утворенні зони інтенсивної тріщинуватості, показана можливість перевірки ефективності заходів зі зміцнення порід на основі математичного моделювання.

Ключові слова: кар'єр, стійкість борту, тріщини, зміцнення порід, метод скінчених елементів, напружено-деформований стан

The manuscript was submitted 29.03.22.